Rafal GAWARKIEWICZ*

AN ATTEMPT AT IDENTIFYING THE INFLUENCE OF TEST HEAD ASSEMBLY STIFFNESS ON THE RESULTS OF A TRIBOLOGICAL EXPERIMENT CONDUCTED UNDER MICRO-OSCILLATION CONDITIONS

PRÓBA IDENTYFIKACJI WPŁYWU CECH SZTYWNOŚCIOWYCH GŁOWICY BADAWCZEJ NA WYNIK EKSPERYMENTU TRIBOLOGICZNEGO W WARUNKACH MIKROOSCYLACJI

Key words:

dry bearing materials, micro-oscillations, experimental investigations, theoretical analyses, simulation

Słowa kluczowe:

bezsmarowe materiały łożyskowe, mikrooscylacje, badania doświadczalne, badania teoretyczne, symulacja

Abstract

The outcome of experimental research on a group of dry bearing materials carried out under small oscillation conditions and using a test rig designed and made at Gdansk University of Technology inspired the decision to find out

* Gdańsk University of Technology, Faculty of Mechanical Engineering, ul. G. Narutowicza 11/12, 80-233 Gdańsk, Poland.

if the stiffness of test head elements influenced the generated results. Therefore, a computer model utilising finite elements was devised and used to simulate the workings of the test head. The model enabled full control of the head's geometry, and loading and boundary conditions at every stage of simulation. Moreover, the simulation includes the preparation of test head elements, fixings, and the specimen loading, and executes the displacement of the counter-face during full-cycle reciprocating motion. Finally, the results of computer simulation are compared with those produced by experimental testing.

INTRODUCTION

Dry bearing materials, working under small oscillation conditions, often show different wear resistance. This is especially true when they operate in a unidirectional motion. It was found **[L. 1, 2, 3, 4]**, when selecting dry bearing materials for applications where small displacement oscillations are prevailing, that it is impossible to employ a standard test (constant reciprocating sliding speed) to assess their fitness for purpose. Therefore, the only way forward was to carry out experiments using a test apparatus especially designed at Gdansk University of Technology **[L. 4]**. Test results indicated that materials with an enhanced ability to elastically deform in shearing have increased wear resistance. This finding suggested that the stiffness of constituent components of the test head might influence the wear performance of the materials tested and provided motivation for the subsequent research presented in this paper.

EXPERIMENTAL RESEARCH

A schematic diagram of the test head is shown in **Figure 1 [L. 4]**. The operation of the head is as follows. A drive shaft with a cam of eccentricity (ε) enforce a reciprocating motion of the follower (P) together with the holder for a steel counter-specimen (denoted PP in **Fig. 1**, see also **Fig. 3**). Two test specimens (upper, U and lower, D) made of dry bearing material are pressed with force N into the counter-specimen holder, which in turn is attached to arms of a special holder (U). Variable friction forces (T_1 and T_2) are produced at the interface between counter-specimen and test specimen. Within the full cycle of motion at the interface, there are periods when there is no sliding and the tested material is subjected to elastic deformation only (e_1 and e_2 as indicated in **Fig. 2**).

After that, the sign of the friction force is reversed and the period of sliding commences. During one cycle of reciprocating motion (cp), the nominal sliding distances are z_1 and z_2.

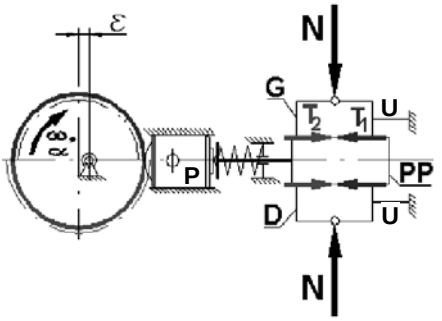

Fig. 1. Test head diagram: G and D – upper and bottom specimen, U – specimen holder, PP – counter-specimen, P – holder follower assembly; α – angle of rotation of drive shaft with an eccentric (ε) cam, N – specimens' loading forces, T_1, T_2 – friction forces

Rys. 1. Schemat ogólny głowicy badawczej: G i D – górna i dolna próbka, U – uchwyt próbek, PP – przeciwpróbka, P – popychacz; α – kąt obrotu wałka z mimośrodem o ekscentryczności (ε), N – siły obciążające próbki, T_1, T_2 – siły tarcia

However, the results suggested that the elastic deformations (e_1 and e_2) effectively reduce the total sliding distance to which test samples were nominally subjected. Consequently, the assumption was made that a part of the total sliding distance during which no relative sliding takes place will be excluded from the estimation of the wear resistance coefficient for dry bearing materials tested under small oscillation conditions **[L. 3, 4]**.

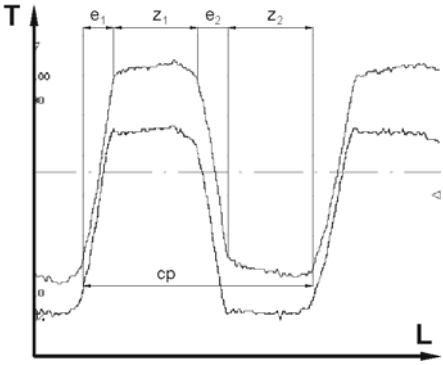

Fig. 2. An example of friction force (T) changes vs. sliding distance (L). Phases of counter-specimen movement relative to specimens (in one cycle *cp*): e_1, e_2 – elastic deformations, z_1, z_2 – sliding

Rys. 2. Przykładowy przebieg siły tarcia (T) w funkcji drogi tarcia (L). Fazy ruchu przeciwpróbki względem próbek (w jednym cyklu wymuszeń *cp*): e_1, e_2 – deformacje sprężyste, z_1, z_2 – poślizg

The extent of the distance taken by elastic deformations as a proportion of the nominal (total) sliding distance was gleaned from the pattern of changes in friction during a test **[L. 3, 4]**. This form of correction is not normally

considered in a typical wear test in which sliding motion is unidirectional and cyclic changes in elastic deformation due to tangential (frictional) loading do not take place. The ability of a test specimen to accommodate motion without relative physical slip at the interface depends mainly on the mechanical properties of specimen's material, its thickness, surface topography, the frictional characteristics of the counterface, the applied load to the contact, the amplitude of reciprocating motion, as well as on the stiffness of the constituent components of the test head.

COMPUTER SIMULATION

The importance of the stiffness of test head's components and its potential influence on experimental results was evaluated through computer simulations of the test rig used in experimental studies **[L. 6]**. A finite element (FE) programme was used to model the operation of the test rig.

The model

The important components of the head assembly are depicted in **Figure 3**.

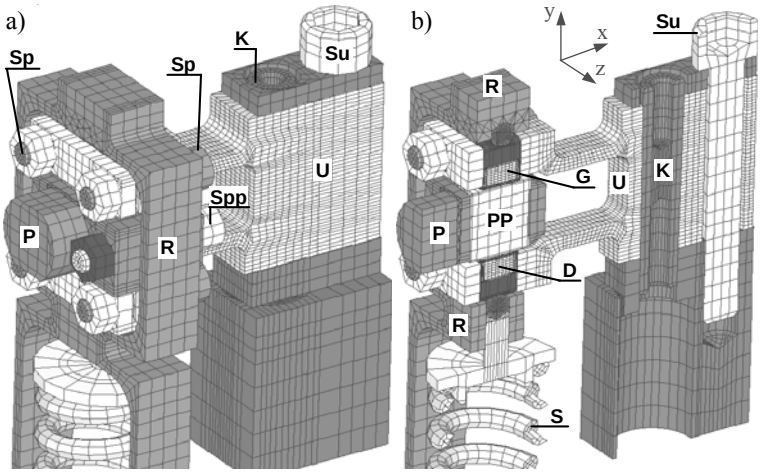

Fig. 3. Main part of the test head assembly: a) general view, b) axial section – details in table 1

Rys. 3. Główna części modelu węzła badawczego: a) w widoku ogólnym, b) w przekroju osiowym – opis w **tabeli 1**

In order to reproduce the working of the test head and to simulate reciprocating motion taking place within the contact region created by the test specimen and its counterface, nine separate simulation stages were identified. They are sequentially presented in **Table 1**. The model includes only these

components of the test head that are in an adjacent space surrounding the specimen/counterface unit or those with the direct influence on the unit. The geometrical model of the head assembly was not imported from any CAD system into the FE programme because of potential difficulties with controlling the process of meshing both in terms of its density the use of element type. Furthermore, imported geometry would make free and full parametrisation of the model impossible. Hence, it was decided to create the geometry of the head assembly utilising ASNSYS Parametric Design Language (APDL). A number of benefits resulted from using APDL such as independent defining and creating contact associations, and the full management of the selection and division of finite elements. As a consequence of adopting this approach, the time of computing was very substantially reduced.

Simulation results

The first step in the simulation procedure consisted in checking that the elements of the mesh were in contact with one another and, afterwards, computation of the reaction forces. The second step (**Table 1**) involved simulation of the peg K movement in order to position specimen holder U at the depth of 0.2 mm measured by the displacement of the peg K in vertical direction. Simulation also involved tightening the screw Spp **(Fig. 3)** to fix the position of the counter-specimen PP in the holder follower assembly P. It was found that the displacement of 2 μm induced by the screw tightening secured proper fixing of the holder. **Figure 4** shows essential elements of the test head

Table 1. Main simulation stages of work of test head one by one
Tabela 1. Zestawienie kolejno głównych etapów symulacji pracy węzła badawczego

Stage	Kind of enforced loading
1	+ initiation of contact elements between elements of test head assembly
2	+ ”driving in” of peg (K) for the specimens holder (U) establishing + ”tightening” of the screw (Spp) for the counter-specimen (PP) fixing in the holder follower assembly (P)
3	+ deleting of boundary conditions (for the "driving in") of the peg (K)
4	+ ”tightening” of the screw (Su) fixing the specimen holder to test head housing + small squeeze of spring (S) for preliminary loading of the specimens (G,D)
5	+ continuation of tension of spring (S) of loading frame (R) to obtain appropriate specimens loading
6	+ ”tightening” of the screws (Sp) for fixing specimens (G, D) + effect of gravitation
7	+ movement of holder follower assembly (P) with counter-specimen (PP) to specimens holder side on distance equal one amplitude of reciprocating motion
8	+ full return of holder follower assembly (P) from specimens holder side
9	+ renewed full movement of holder follower assembly (P) with counter-specimen (PP) to specimens holder (U) side

after the second step in the simulation process. It can be seen that the specimen holder was unevenly displaced in the X-direction. The upper test specimen was moved to the counter-specimen by 5 μm while the lower test specimen moved less than 3 μm. This is most probably due to the cone-shaped push-in type of connection.

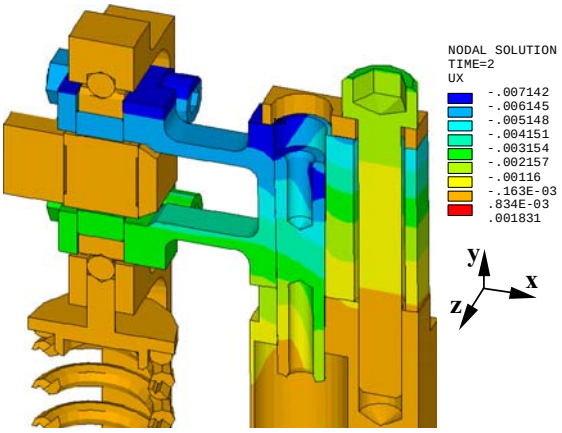

Fig. 4. Distribution of X direction displacements [mm] of elements of test head after 2nd stage (according to the Table 1)

Rys. 4. Przemieszczenia [mm] w kierunku osi X w elementach węzła badawczego po 2. etapie obciążenia (według **tabeli 1**)

During the third step of simulation, constrains imposed on the peg were gradually relaxed as, in reality, the adjustment of the peg takes place through haphazard turning of the screw. Therefore, it is vital to ensure that the depth

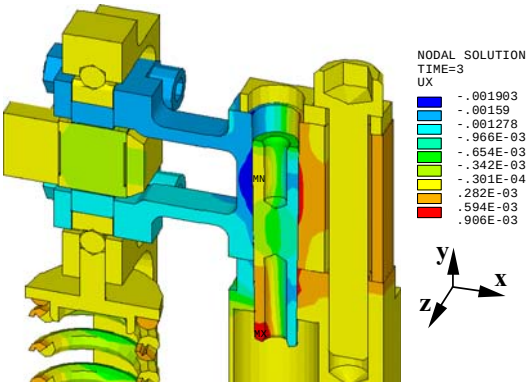

Fig. 5. Distribution of X direction displacements [mm] of elements of test head after 3rd stage (according to the Table 1)

Rys. 5. Przemieszczenia [mm] w kierunku osi X w elementach węzła badawczegopo 3. etapie obciążenia (według **tabeli 1**)

at which the peg was positioned is the same as the depth measured experimentally. As expected, removal of constraints resulted in a backward movement of the peg equal to about 5 μm. Furthermore, the relaxation of peg's constraints reduced the difference in the location between test specimen and counter-specimen to about 1 μm as shown in **Figure 5**.

In the fourth step of simulation, the tightening of the screw (denoted Su in **Figure 3**) to fix the specimen holder (U) in the test head was considered. Additionally, initial tensile loading of the frame (R) by a small compression spring (S) was included, because this enabled the test specimen to self-adjust to the counter-specimen. The degree to which the specimen's holder screw was tightened manifested itself by its elongation of about 2 μm.

All contact interactions between components of the test head were modelled with appropriate contact elements, which resulted in simulated behaviour similar to that encountered in reality.

Figure 6 illustrates the distribution of displacements in the X-direction produced by the fourth step of simulation during which the same operating conditions were maintained for both test specimens. In order to get the necessary loading of test specimens, a required tension of the spring (S in **Figure 3**) in the loading frame (R) was estimated during the fifth step of simulation. In the sixth step of simulation both test specimens (G and D) were fixed in their positions at the ends of the specimen holder (U). In addition, gravitational forces were also included, although their significance was quite minute as confirmed by the simulation results.

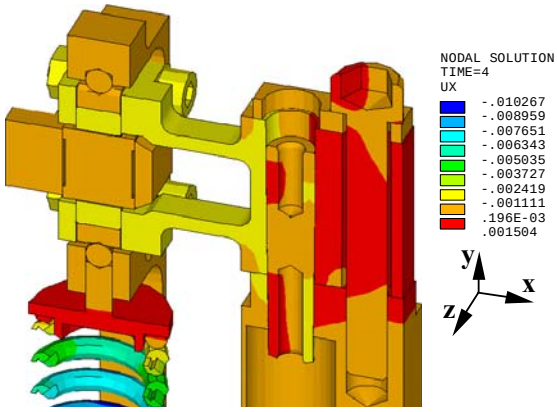

Fig. 6. Distribution of X direction displacements [mm] of elements of test unit after 4th stage (according to the Table 1)

Rys. 6. Obraz przemieszczeń [mm] na kierunku osi X w elementach węzła badawczego po 4. etapie obciążenia (według **tabeli 1**)

The seventh step of simulation involves the main phase of the operation of the whole test unit. The shift of the counter-specimen relative to the specimen holder was 120 μm as shown in **Figure 7**. In the eighth and ninth steps of the simulation, a full reciprocating motion of the counter-specimen was incorporated. The stroke was equal to 240 μm as illustrated in **Figure 8**. It was found that the specimen holder moves about 2 μm in the X-direction in response to the displacement of the counter-specimen. This indicates that the elastic deformation within the specimen holder assembly is about 8 μm when the reciprocating motion of the counter-specimen is 480 μm. In practical terms, it means that the actual sliding distance is reduced by about 1.7%.

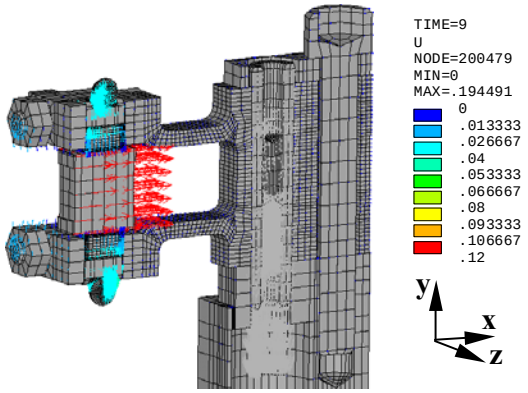

Fig. 7. Global displacements [mm] of elements of test unit after 7th stage (according to the Table 1)

Rys. 7. Całkowite przemieszczenia [mm] w elementach węzła badawczego po 7. etapie obciążenia (według **tabeli 1**)

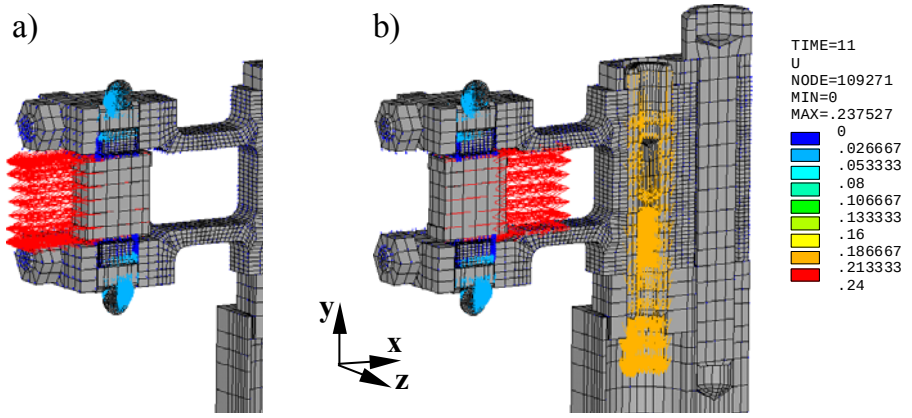

Fig. 8. Global displacements [mm] of elements of test unit after 8th (a) and 9th (b) stage (according to Table 1)

Rys. 8. Całkowite przemieszczenia [mm] w elementach węzła badawczego po: 8. (a) i 9. (b) etapie obciążenia (według **tabeli 1**)

DISCUSSION OF RESULTS

In order to define the stiffness properties of components involved in sliding, a diagram depicting changes in the friction force with the nominal sliding distance was constructed **(Figure 9)**. In this figure, changes in the friction force produced by the simulation are compared with those measured experimentally for a self-lubricating material, Devatex **[L. 7]**, which is free of the stick-slip phenomenon. The counter-specimen was made of a steel.

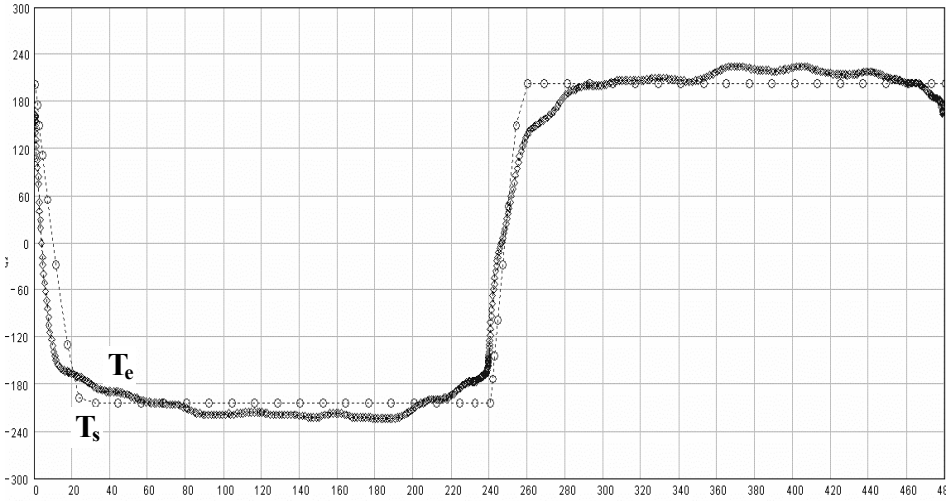

Fig. 9. Friction force [N] changes vs. nominal sliding distance [μm] obtained: T_e – experimentally, T_s – from simulation

Rys. 9. Przebieg siły tarcia [N] w funkcji nominalnej drogi tarcia [μm] uzyskany: T_e – eksperymentalnie, T_s – z symulacji numerycznej

Gradients of the two curves shown are undoubtedly different and illustrates that the stiffness of the elements involved in sliding motion plays an important role in the whole process. Besides, it is apparent that the stiffness characteristics of the elements holding test specimens are not equal during the full cycle of reciprocating motion of the counter-specimen.

Another matter concerns the changes in friction force during the full cycle of reciprocating sliding. They are entirely different, but that issue is not the main purpose of this paper. Modelling of an actual sliding distance, the main aim of this paper required the assessment of the relative displacement occurring between the test specimen and counter-specimen and excluding input from kinematic friction. A theoretical model of the transition from a static friction to kinematic friction required the estimation of the static friction coefficient. For the initial phase of the test, it was assumed that static friction coefficient equals the kinematic friction coefficient for tested dry bearing

material. The assumption was made based on the test results produced by the rig having the head that is the subject of the computer simulation presented here.

SUMMARY

There are many reasons for experimentally observed differences in friction force changes and those produced by computer simulations. Some of them may be attributed to certain simplifications embedded into the computer model. Nonetheless, results of computer simulations provide a basis for the following conclusions.

- The stiffness of test head components have an influence on the experimental results generated during testing.
- The flexibility of elements clamping test specimen reduce the real sliding distance measured relative to the counter-specimen. As a consequence, the sliding distance is reduced by about 1.7% and so is the observed wear rate.
- The magnitude and distribution of stresses in the components of the test head are both within safe limits.

REFERENCES

1. Lancaster J., et al.:, Effects of amplitude of oscillation on the wear of dry bearing containing PTFE. Transaction of ASME – Journal of Lubrication Technology 1982, Vol. 104, No. 4.
2. Moss B., Hatem B.: Grease Free Bearing Comparison Test on a 300 MW Pump Turbine at Dinorwig Power Station, 2003: http://tss-static.com/remotemedia/media/globalformastercontent/industries/orkot_hydro_2/pdfs_1/Dinorwig_1.pdf.
3. Gawarkiewicz R.: Problem wyboru bezsmarowego materiału ślizgowego dla łożysk pracujących w warunkach małych oscylacji. Tribologia – Teoria i Praktyka nr 211 (2007), pp. 57–69 (in Polish).
4. Gawarkiewicz R., Wasilczuk M.: Wear measurements of self lubricating bearing materials in small oscillatory movement. An International Journal on the Science and Technology of Friction, Lubrication and Wear, Vol. 263 (2007), pp. 458–462.
5. Olszewski O., et al.: Prognozowanie trwałości skojarzeń ślizgowych w warunkach występowania drgań. Report from researches financed by the Polish Committee of Scientific Research, project No No. 7T07C 008 17, Politechnika Gdańska, Gdańsk 2000 (in Polish).
6. Gawarkiewicz R., et al.: Analiza właściwości tribologicznych wybranego bezsmarowego materiału łożyskowego w warunkach mikrooscylacji stycznych w płaskim skojarzeniu ślizgowym. Report from researches financed by the Polish Committee of Scientific Research, project No. 4 T07B 06328, Politechnika Gdańska, Gdańsk 2007 (in Polish).
7. http://deva.de/en/product-range/deva-tex.

Streszczenie

Po badaniach tribologicznych grupy bezsmarowych materiałów łożyskowych w warunkach małych oscylacji, na specjalnie wykonanym w Politechnice Gdańskiej stanowisku badawczym, postanowiono zbadać, czy sztywność elementów głowicy badawczej wpływa na otrzymany wynik eksperymentu. W tym celu przeprowadzono komputerowe symulacje pracy węzła badawczego, wykorzystując metodę elementów skończonych. Model stworzono w taki sposób, aby była możliwa pełna kontrola jego geometrii, obciążenia, warunków brzegowych – i to na każdym etapie symulacji. Badania teoretyczne objęły etapy przygotowania elementów głowicy badawczej do testu, mocowania próbek oraz przeprowadzenie pełnego cyklu ich współpracy z przeciwpróbką w ruchu posuwisto-zwrotnym. Na koniec porównano otrzymane wyniki z wynikami z badań doświadczalnych.